BNL-113384-2016-TECH
C-A/AP/579;BNL-113384-2016-IR

Report on LEReC Recombination Monitor APEX Study on June 15th 2016

A. Drees

December 2016

Collider Accelerator Department
Brookhaven National Laboratory

U.S. Department of Energy
USDOE Office of Science (SC), Nuclear Physics (NP) (SC-26)

DISCLAIMER

BNL-113384-2016-IR

C-A/AP/579
December 2016

Report on LEReC Recombination Monitor APEX Study June 15th 2016

Drees, D. Bruno, T. Curcio, C. Montag, G. Robert-Demolaize, P. Thieberger

Collider-Accelerator Department
Brookhaven National Laboratory
Upton, NY 11973

U.S. Department of Energy
Office of Science, Office of Nuclear Physics

Report on LEReC Recombination Monitor APEX study June 15th 2016

A. Drees, D. Bruno, T. Curcio, C. Montag, G. Robert-Demolaize, P. Thieberger

December 21, 2016

1 Motivation

During the prospective Low Energy RHIC electron Cooling (LEReC) operation, the electron beam will overlap and interact with the low energy ion beam to provide transverse cooling. Cooling is needed to facilitate reaching the BES-2 (Beam Energy Scan 2) program goals of an average store luminosity of 5×10^{24} cm^{-2} s^{-1} at 3.85 GeV/n and 17.3×10^{24} cm^{-2} s^{-1} at 9.1 GeV/n. The RHIC phase of BES-2 is currently planned for the RHIC runs in 2019 and 2020.

Effective cooling will depend on the accuracy of velocity matching between the two beams. Another process, the rate of ion-electron recombination, is also maximized when the velocities are matched but the exact matching requirement is less stringent. Therefore, as suggested by one of us, detecting and maximizing recombination signals should be helpful in finding the narrow velocity matching window conducive to cooling [2].

When $^{197}Au^{79+}$ RHIC ions pick up an electron from the LEREeC electron beam they are converted into $^{197}Au^{78+}$ ions with nearly the same momentum while having about 1.3% higher magnetic rigidity than the original $^{197}Au^{79+}$ particles. The detection of the recombined ions can be done by driving the $^{197}Au^{78+}$ beam into the beam pipe wall, creating showers of secondary particles which then can be detected outside the cryostat by using appropriately positioned detectors. For the purpose of forcing losses of the expected off-momentum particles a dedicated lattice with large horizontal dispersion in one arc was proposed and designed [2].

2 Recombination Monitors

Four Pin Diodes and two plastic scintillators with PMTs were installed close to Q15 in the yellow sector 1 arc (Y1). Both detector types were installed in the shutdown before run16 and were made available by the instrumentation group. Fig. 1 shows the array of detectors in the tunnel. The first device is one of the two identical scintillators followed by two pin diodes, the second scintillator and another pair of pin diodes. The diameter of the scintillator is 5 cm. While both detector types serve as loss monitors, the sensitive areas of the two are quite different: 7.34 mm^2 for the PDs and 1962.5 mm^2 for the scintillators, a difference of about a factor 270. The side-wide-names and s-locations for the 6 devices are as listed in Tab. 1.

It turns out that the small size of the PDs rendered them unfit for this study due to the low counting rate.

Figure 1: Array of PDs and scintillators installed in the Yellow sector 1 arc.

SWN	**s-location [m]**
y1-pmt15.1	2,321.9
y1-pd15.1	2,321.2
y1-pd15.2	2,319.6
y1-pmt15.3	2,317.7
y1-pd15.3	2,317.0
y1-pd15.4	2,315.2

Table 1: List of installed pin diodes (pd) and scintillators (pmt).

3 What Do we need?

The specially designed lattice involved re-purposing some of RHIC's γ_T quadrupoles as a prerequisite and parts of the needed installations were done before the RHIC run started. However, given that the γ_T's were in use for each and every Au fill during run 16, considerable time overhead (about 3 h) for re-cabling had to be allocated before and after an APEX session in which this lattice was actually supposed to be used. Therefore, to minimize the need for dedicated time, the recombination monitor testing was essentially split into two parts:

(I) show that off-momentum $^{197}Au^{78+}$ particles are lost at locations with dispersion and can be distinguished from $^{197}Au^{79+}$.

(II) demonstrate that shower particles from 3.85 GeV/n beam ions can be detected outside the cryostat.

Part I could be done parasitically during physics stores. All we needed were detectors in areas with dispersion. Many standard loss monitors as well as the newly installed recombination scintillators and PDs all fit this bill.

4 Dispersive Losses

During the 2016 AuAu run we could see plenty of dispersive losses in RHIC. Dispersive losses were visible due to the prefire protection bumps in two arcs (sector 10 in blue and sector 9 in yellow before April 5th and sector 3 in blue after April 5th). The protection bump amplitude has a 20 mm maximum. Fig. 2 shows a snapshot of a loss pattern from about 2 hours into store 19699 (before Apr 5th). The black line corresponds to the loss rate, measured by a standard RHIC BLM, as a function of location s(m). The loss levels in units of rad/h are normalized to the maximum of this distribution. For the normalization (and the depiction) all losses in the collimator area are suppressed (between sector 7 Q4 and sector 8 Q4). For this data set the maximum of approximately 24 rad/h appeared to be at s = 1523.4 m. This location corresponds to g10-lm16, a part of the blue protection bump. This is not, however, the location of the largest amplitude of the protection bump. The simulated expected loss

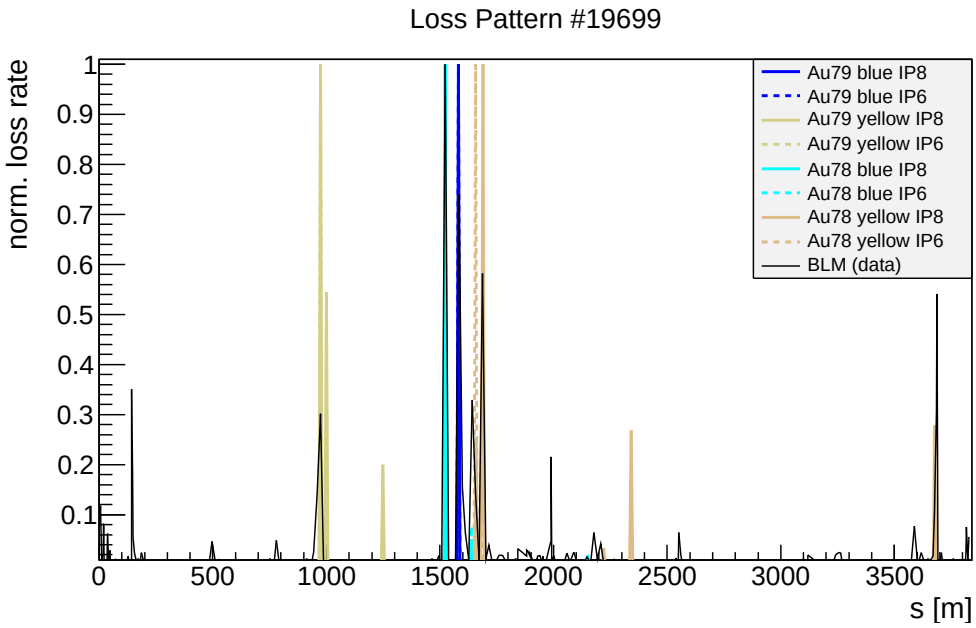

Figure 2: Comparison of predicted losses of $^{197}Au^{78+}$ and $^{196}Au^{79+}$ with BLM data from store 19699, approximately 2 h after reaching store. Losses at the collimators are suppressed.

levels [1] are shown here in appropriate colors (for specifics please refer to legend in Fig. 2). Predictions were made for 8 cases: loss distributions of $^{197}Au^{78+}$ and $^{196}Au^{79+}$ isotopes[1] created in either IP6 or IP8 and then tracked in the yellow or blue ring respectively. Each simulated data set is normalized to its individual maximum. Loss predictions for $^{197}Au^{78+}$ are about a factor 10 higher than expectations for $^{196}Au^{79+}$ and about a factor 10 higher for blue than for yellow regardless of the source. The data does not reproduce such big difference between the two sources of Au ions. However, due to the normalization, this is not reflected in the shown peak amplitudes. Two small peaks in the data are not reproduced by a peak in the simulations. The 20% loss peak around s = 2000 m is at the location of the blue polarimeters, perhaps due to a small pressure bump. The loss peak around s = 140 m is at the blue injection kickers (the equivalent of the losses at the yellow injection kickers at s =

[1] generated from electromagnetic dissociation associated with the Au-Au collisions at IPs

3690 m). In the simulation, blue $^{197}Au^{78+}$ ions created in IP8 would contribute to it but they are expected to get lost in the blue protection bump area around s = 1600 m before they reach the injection kickers. Data suggests that either not all get caught in the protection bump or some blue $^{197}Au^{78+}$ ions created in IP6 might contribute.

Fig. 3 shows the loss pattern in the sector 10 arc at the beginning of store 19704 on March 17th, just before the diode failure. Superimposed with the same scale on the x-axis is an image containing the closed orbit according to the model and the horizontal dispersion for the two different types of off-momentum ions ($^{197}Au^{78+}$ and $^{196}Au^{79+}$). It supports the

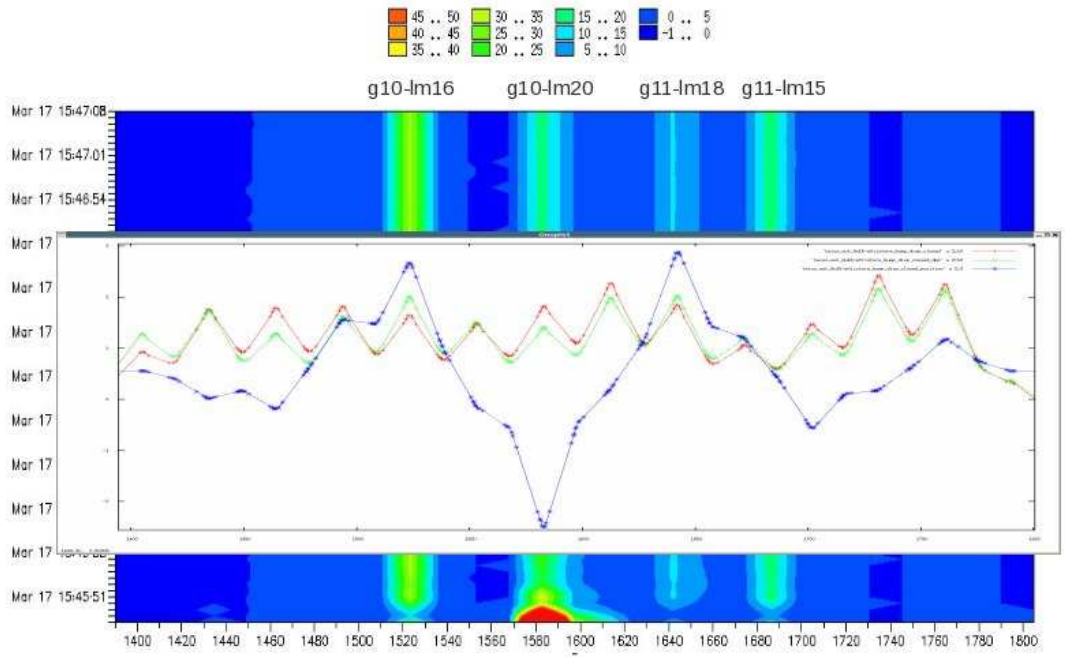

Figure 3: Au-Au Loss pattern in the sector 10 arc at the beginning of store 19704. The overlapping image contains the model closed orbit (blue) and the horizontal dispersion for $^{196}Au^{79+}$ (red) and $^{197}Au^{78+}$ (green).

conclusion that the losses at g10-lm16 and g11-lm18 are from superimposed closed orbit and dispersion bumps in the blue ring while g10-lm20 is caused by the bump amplitude maximum alone. The losses in g11-lm15 can be attributed to the yellow beam.

Figure 4 shows the yellow injection area in sector 5 from s = 3500 m to the center of IP6. The data in the graph, shown as a blue line and blue dots, are from BLMs. The data is a snapshot from about 10 s after the beginning of collisions in store 20202. At the time Au-Au collisions at 100 GeV per beam were provided. The loss rates are scaled with a factor of 0.12 to be shown together with the dispersion function. The dispersion function is shown as a red line. Beam direction is from right to left. Coming from IP6, particles get lost as soon as the dispersion function reaches a value larger than 1.1 m. This is reflected in the large peak at about s = 3680 m, in the area of the yellow injection kickers. Most particles are lost at the first opportunity and no further peaks are visible. This loss pattern is typical for all AuAu stores and supports the notion of dispersive losses.

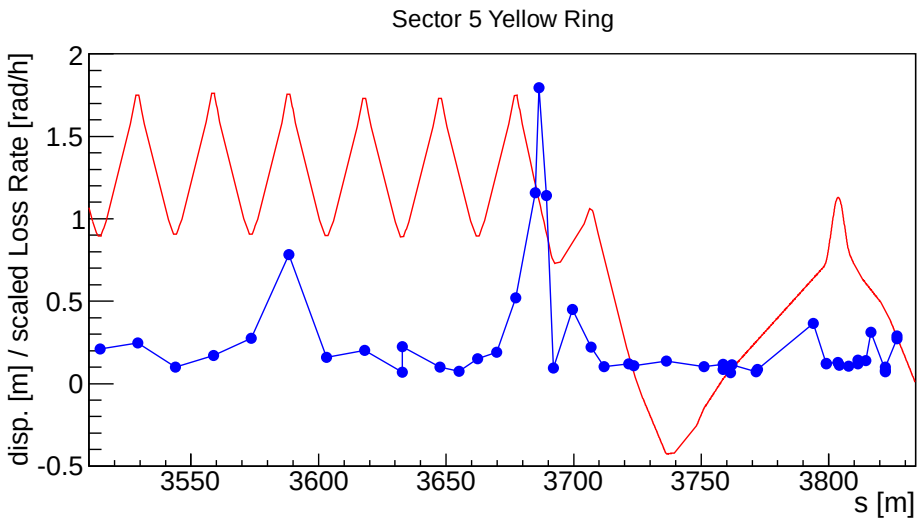

Figure 4: Dispersion function (red line) and measured loss rates (blue dots and line) from fill 20202 in 2016 in the yellow injection area (sector 5).

5 $^{197}Au^{78+}$ Production in Au-Au Collisions

So far we have seen dispersive losses with standard BLMs in areas with large closed orbit bumps or significant increase in the dispersion function (i.e. the Q9 area outside the low beta insertions). In general, dispersive losses can be produced by any type of off-momentum $^{197}Au^{79+}$ or from $^{197}Au^{78+}$ and $^{196}Au^{79+}$. $^{197}Au^{78+}$ is produced in Au-Au collisions by recombination after Bound Free Pair Production which has been observed earlier in RHIC during the 2005 CuCu run [3]. Therefore it is expected that $^{197}Au^{78+}$ losses follow the collision rate at the experiments. During run 16, the collision rate in STAR was leveled to 65 kHz, while the collision rate in PHENIX remained maximized throughout the stores. The top graph of Fig. 5 shows BLM signals and collision rates from the two experiments for store 19812. The two loss monitors chosen are both from the yellow injection kicker area with g5-lm9.2 located at s = 3689.4 m and g5-lm9.3 three meters further downstream at s = 3686.5 m. The first loss monitor is mounted between the first and second injection kicker modules. The second loss monitor is mounted alongside the center of the fourth and last injection kicker module. The g5-lm9.2 signal (red line) resembles strictly the collision rate evolution from the STAR detector, while the signal from g5-lm9.3 (green line) does not. After an initial decay that resembles the evolution of the PHENIX ZDC rate it shows a steep climb just before 1:30. No apparent reason for this increase could be found (i.e. no significant orbit change, no pressure change, no increase in beam decay). After 1:45 the signal keeps to decrease more or less at a rate resembling the PHENIX ZDC signal, however, it does not show the same mild increase after 4:00. Therefore the resemblance is likely more a coincidence and not cause and effect. However, this is different for the STAR collision rate and the loss rate seen by g5-lm9.2. The constant ratio of the STAR collision rate and the g5-lm9.2 loss rate is depicted in the lower plot. A constant fit to the data yields a ratio of 9.3 kHz per rad/h. This ratio is maintained throughout all stores and only changes by about 10% after the beam induced vacuum leak on April 29th.

In order to determine if there is a significant component from PHENIX collisions in the g5-lm9.3 signal we compared it to the PHENIX collision rate during a vernier scan. The result

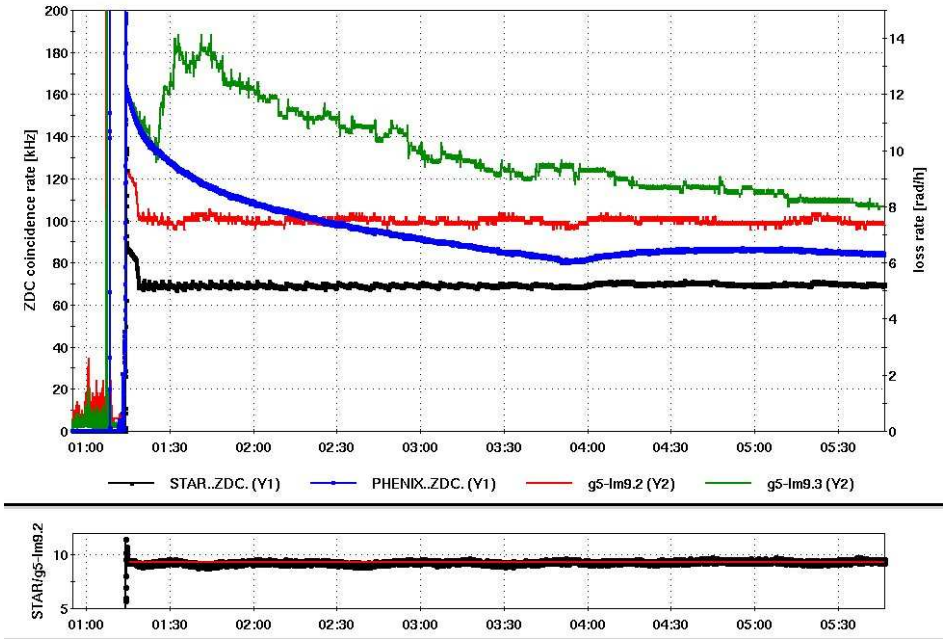

Figure 5: Top: Signals from two consecutive loss monitors in the injection kicker area (sector 5) and the ZDC collision rates from STAR and PHENIX during fill 19812. Bottom: ratio of STAR's ZDC coincidence rate and g5-lm9.2 loss monitor with a constant fitted to the data.

is shown in Fig. 6. While the vernier scan is going on, the collision rate is changed in steps from fully overlapping to fully separated by transversely scanning one beam with respect to the other. The change in collision rate clearly affects g5-lm9.3 while it does not have any impact on g5-lm9.2. The vernier scan is done in two parts: vertical first, then followed by horizontal. In this particular case the yellow beam is moved by up to +/- 0.65 mm in each plane, causing the typical pattern of four steps. When the beams are separated vertically, the losses decrease with the collision rate, if only by a much reduced amount. When the beams are separated in the horizontal plane, the loss rate increases at first (while the beams are moved to +0.65 mm) and then decreases. At this point we don't have an explanation for this behavior.

5.1 $^{197}Au^{78+}$ Signal from Recombination Monitor Scintillators

The dispersive $^{197}Au^{78+}$ losses are also visible in the middle of the arc where the recombination monitor scintillators were installed downstream of the yellow sector 1 Q15 magnet. Fig. 7, left, depicts the loss rate seen by y1-pmt15.1 during an ongoing vernier scan in IP8. During the course of a vernier scan the Au-beams are step-wise brought out of and back into collision at one IP. The loss signal clearly tracks the collision rate as measured by the "PHENIX..ZDC" signal, i.e. the ZDC coincidence rate. Note that at the same time collisions are still provided at the STAR IP at rates between 70 kHz and 78 kHz.

Similarly, the recombination monitor rates are jumping up as soon as the separation bumps are being collapsed during the storage ramp, as shown in Fig. 7, right. The storage ramp start and end are indicated by the red and purple vertical lines. The scintillator signal clearly follows the evolution of the collision rates. Shown here are the STAR ZDC

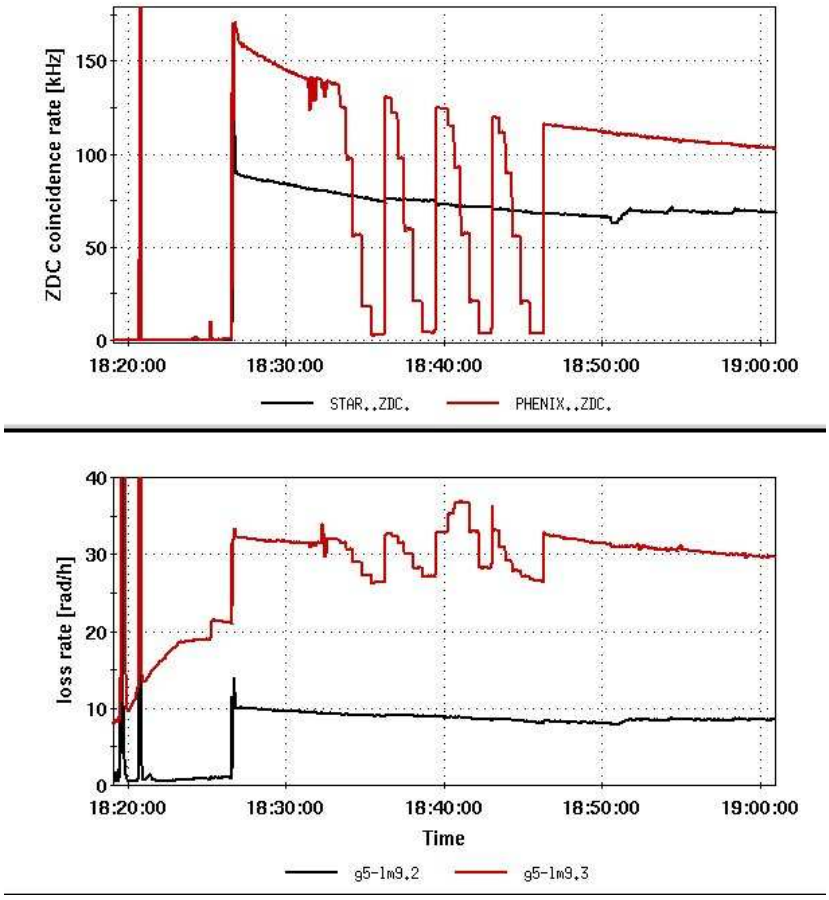

Figure 6: Top: STAR and PHENIX ZDC coincidence rates during the first hour of store 19874. Bottom: Signals from g5-lm9.2 and g5-lm9.3 during the same time.

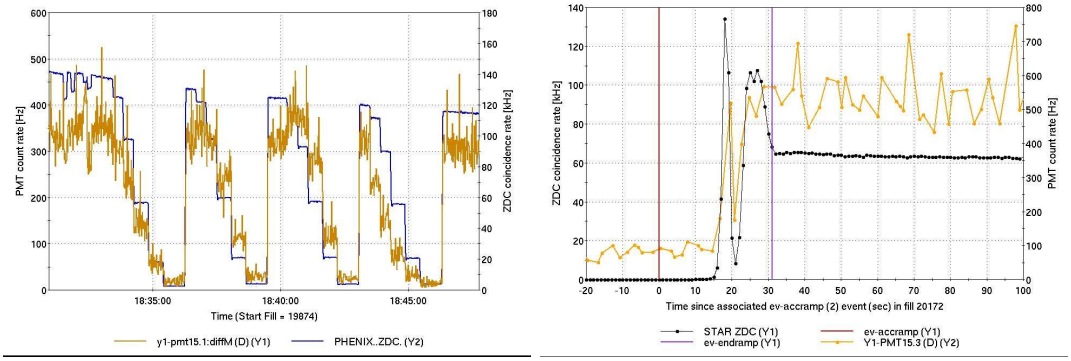

Figure 7: Left: Recombination scintillator signal and PHENIX ZDC coincidence rate during the 19874 vernier scan. Right: Recombination scintillator signal and STAR ZDC coincidence rate during the storage ramp and onset of physics collisions in store 20202.

coincidence rates. Both plots in Fig. 7 provide convincing evidence that $^{197}Au^{78+}$ ions are created in collisions and are being lost in areas with horizontal dispersion such as the middle of an arc. The installed scintillators are well equipped to capture such loss signals.

6 APEX session June 15th

6.1 RHIC Setup

Beam studies with Au at 3.85 GeV in the yellow ring were performed between 11:30 and 15:45 during fill 20159. The time from 8:00 to 11:30 was used to set RHIC up for low energy at 3.85 GeV. Before injection we ramped from "Park" (50 A) to 3.85 GeV (181 A) by using the ramp file dAu16-4GeV.

The plan for study was as follows:

- In order to force losses in the area put the closed orbit near the aperture at Y1Q14 at s = 2339 m, 17 m upstream of the scintillator. This was achieved by adding an approx. 17 mm horizontal bump in that area.
- Excite the beam with Artus kicks with the goal of creating sharp instantaneous losses and comparing that with the rates from the recombination monitors (removes the effects of the large, slow steady state losses).
- Repeat with the bump moved in s coordinate by 30 m to Y1Q12 at s = 2369 m.

Once RHIC was set up for 3.85 GeV operation the yellow ring was filled repeatedly

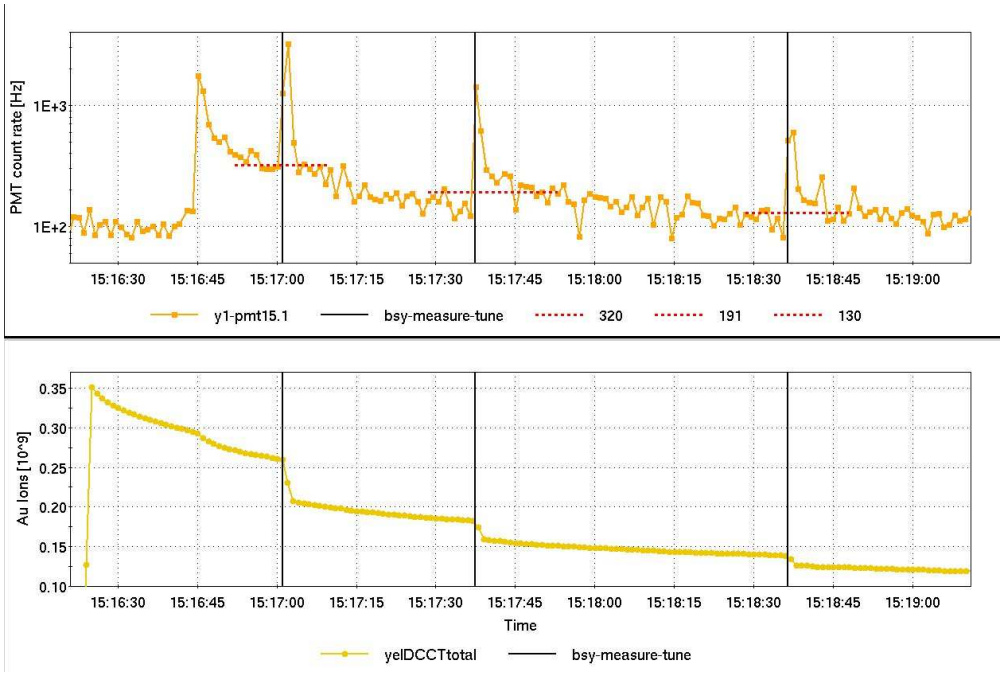

Figure 8: One PMT calibration data set with three tune meter kicker triggers. Top: PMT count rate, bottom: beam intensity.

with 6 bunches for a series of short "stores" . One of the six bunches was then excited using the resonant tune meter kicker. Due to the large beam size and the horizontal bump

in the arc, each tune meter trigger caused a certain amount of beam loss associated with a spike in the PMT count rate. One example raw data set is shown in Fig. 8.

The vertical black lines indicate a tune meter trigger, causing a varying amount of beam loss (bottom), associated with a spike in the PMT count rate (top). Since there is visible beam loss in the arc even without excitation, a baseline, indicated here by a red dashed line, for each individual trigger is subtracted from the PMT peak value.

6.2 Analysis

The Y1 arc with its large horizontal bump is not the only loss location and some beam is getting lost at other places in the ring, mostly at the collimators. Therefore, in order to calculate the amount of beam lost close to the PMT, the beam loss on the collimators had to be subtracted from the beam loss as seen in Fig. 8, bottom. For this purpose the loss rate on the collimator PDs was calibrated in a similar manner as described above. Several data points were taken with the 3.85 GeV beam by means of excitation with the tune meter kickers. The result is shown in Fig. 9. The data set shown here was taken without a bump

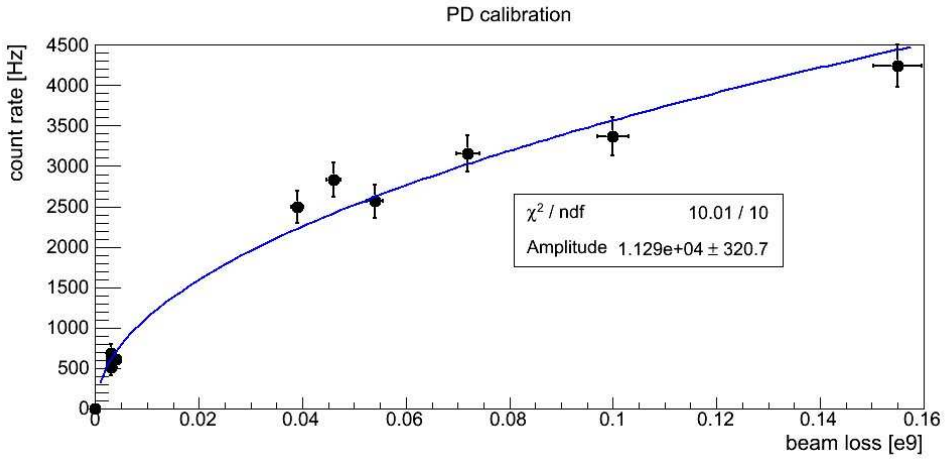

Figure 9: Loss rate measured by the PDs per amount of beam lost on the collimators.

in the Y1 arc and most if not all beam is assumed to be lost on the collimators. Even though a linear correlation was expected, the fit function $R_{PD} = A \times \sqrt{I_{lost}}$ was chosen because it obviously describes the data much better and thus would enhance the accuracy of the correction. However, at this point it is not understood why the data does not favor a linear correlation. The fit is shown as a blue line, with the fitted Amplitude A = 1.13 $\times$ $10^4[Hz/1e9]$. The correlation and fitted amplitude was used in the following to calculate the correction to the total beam loss as seen by the DCCT.

Fig. 10 shows two data sets with the bump centered at Y1Q14 (black data points) and at Y1Q12 (red data points). The total beam loss is corrected for losses on the collimators as described above. The data quality of the set with the bump centered at Y1Q14 is relatively poor while the other set, with the bump moved upstream by 30 m to Y1Q12, reflects a convincing linear correlation of loss rate vs. beam loss. The calibration factors, assuming a linear correlation, yield:

- Y1Q14: 217,400 cts per 1 $\times$ 10^9 lost Au ions

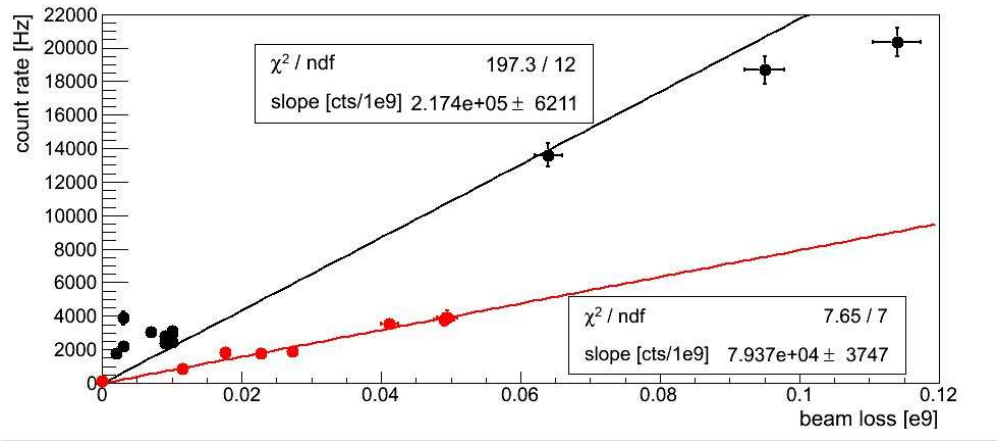

Figure 10: Loss rate measured by the recombination monitor PMT per amount of beam lost in the Y1 arc bump.

- Y1Q12: 79,400 cts per 1 $\times 10^9$ lost Au ions

As expected, the rate on the monitors can be manipulated by controlling the loss location. A move of 30 m reduces the count rate by approximately a factor 3. Considering a $\frac{1}{r^2}$ law and a value of 17 m for r at the Y1Q14 location versus 47 m at the Y1Q12 location, one would expect a reduction of approximately a factor 7, i.e. there is a missing factor of 2.5. However, given the poor quality of the first data set (bump at Y1Q14), this is not too surprising.

7 Conclusion

For AuAu operation at 100 GeV/beam it could be shown that $^{197}Au^{78+}$, once created, can be detected outside the vacuum pipe at locations with significant dispersion (about 1 m and above). $^{197}Au^{78+}$ ions are continuously created in collisions and losses are concentrated in dispersive areas with a small aperture (such as the injection kicker area) or large horizontal orbit deviations (such as the prefire protection bumps). Loss locations can be predicted with reasonable accuracy and the $^{197}Au^{78+}$ signal can be distinguished and separated from the one generated by $^{197}Au^{79+}$.

For AuAu operation at 3.85 GeV it could also be shown that Au ions can be detected outside the beam pipe and the cryostat. Detectors with a larger surface area such as the plastic scintillators with approximately 2000 mm^2 are much better suited to detect the signals (compared to the much smaller PDs). A larger scintillator would give better results. For the existing PMTs we measured a rate of 220 cts per 1 million lost Au ions for a loss location of 17 m upstream of the detector. When the loss location was moved upstream by 30 m, a loss rate of 80 cts per 1 million lost Au ions could be achieved. The results are within a factor 2.5 of a strict $\frac{1}{r^2}$ law, likely due to the poor quality of the first data set. In order to confirm, we suggest to repeat the measurement in FY2017. However, assuming a $\frac{1}{r^2}$ dependence, moving the loss location closer to a future recombination monitor would further increase the yield of detected $^{197}Au^{78+}$ ions. This increase could reach up to two orders of magnitude for a loss location of a few meters upstream of a future recombination detector.

References

[1] Y. Luo et al., "CALCULATION OF PARTICLE LOSS MAPS FOR THE 2016 RHIC GOLD-GOLD RUN", submitted to IPAC2017.

[2] F. S. Carlier, "Detectors for low energy electron cooling in RHIC", C-A/AP/557 CAD technical note, BNL-111866-2016-IR, Feb. 2016.

[3] R. Bruce, J. M. Jowett, S. Gilardoni, A. Drees, W. Fischer, S. Tepikian, and S. R. Klein, "Observations of beam losses due to bound-free pair production in a heavy-ion collider", Phys. Rev. Lett.99, 144801 (2007)